LAWRENCE
LIVERMORE
NATIONAL
LABORATORY

UCRL-JRNL-234156

Highly Potent, Water Soluble Benzimidazole Antagonist for Activated α4β1 Integrin

R. D. Carpenter, M. Andrei, E. Y. Lau, F. C. Lightstone, R. Liu, K. S. Lam, M. J. Kurth

August 30, 2007

Journal of Medicinal Chemistry

Highly Potent, Water Soluble Benzimidazole Antagonist for Activated $\alpha_4\beta_1$ Integrin

Richard D. Carpenter,[†] Mirela Andrei,[‡] Edmond Y. Lau,[§] Felice C. Lightstone,[§] Ruiwu Liu,[‡] Kit S. Lam,[‡,] Mark J. Kurth,[†,*]*

[†]Department of Chemistry, University of California, Davis, Davis, CA, 95616.

[‡]Division of Hematology and Oncology, Department of Internal Medicine, UC Davis Cancer Center, University of California, Davis, Sacramento, CA 95817

[§]Chemistry, Materials, and Life Sciences Directorate, Lawrence Livermore National Laboratory, 7000 East Ave., Livermore, CA 94550

kit.lam@ucdmc.ucdavis.edu, mjkurth@ucdavis.edu

RECEIVED DATE (to be automatically inserted after your manuscript is accepted if required according to the journal that you are submitting your paper to)

Kit S. Lam: Telephone: (916) 734-8012, FAX: 916-734-7946; Mark J. Kurth: Telephone: (530) 752-8192, FAX: (530) 752-8995.

Abbbreviations: PK, pharmacokinetics; HOBt, hydroxybenzotriazole; DIC, 1,3-diisopropylcarbodiimide; DMF, *N*,*N*-dimethylformamide; HBTU, 2-(1*H*-Benzotriazol-1- yl)-1,1,3,3-tetramethyluronium hexafluorophosphate; DIEA, diisopropylethylamine; TFA, trifluoroacetic acid; BSA, bovine serum albumin; PBS, phosphate buffered saline; DOTA, 1,4,7,10-tetracetic acid.

Abstract

The cell surface receptor $\alpha_4\beta_1$ integrin, activated constitutively in lymphoma, can be targeted with the bisaryl urea peptidomimetic antagonist **1** (LLP2A). However, concerns on its preliminary pharmacokinetic (PK) profile provided an impetus to change the pharmacophore from a bisaryl urea to a 2-arylaminobenzimidazole moiety resulting in improved solubility while maintaining picomolar potency [**5** (KLCA4); IC_{50} = 305 pM]. With exceptional solubility, this finding has potential for improving PK to help diagnose and treat lymphomas.

Introduction

The integrin family of membrane proteins, comprised of 24 noncovalent heterodimeric combinations employing 18 α- and 8 β-glycoproteins, are cell surface receptors that respond to and modulate a broad array of extracellular matrix proteins.[1] Specifically, $\alpha_4\beta_1$ integrin regulates lymphocyte trafficking as well as homing in normal adult cells,[2,3] while the activated form of $\alpha_4\beta_1$ regulates tumor growth, metastasis, and angiogenesis, as well as promotes the dissemination of tumor cells to distal organs while facilitating tumor cell extravasation.[3-10] This activated $\alpha_4\beta_1$ integrin is expressed in patients with leukemias, lymphomas, melanomas, and sarcomas;[3] it appears to inhibit apoptosis in malignant chronic lymphocytic leukemias (B-CLL) cells.[6]

Through the use of one-bead one-compound (OBOC) combinatorial library methods,[11,12] we recently reported the discovery of the bisaryl urea peptidomimetic **1** (LLP2A; see Figure 1)[13-15] as a highly potent and selective ligand for the activated form of $\alpha_4\beta_1$ integrin. We further demonstrated that **1** labeled with near-infra red fluorescent dye, can target lymphoma xenograft with high specificity, making **1** a good candidate for the development of lymphoma imaging and/or therapeutic agents. Although the water solubility of **1** when conjugated to a hydrophilic linker is good, **1** by itself is not very water soluble. Furthermore, in vivo optical and radioimaging studies in a xenograft model showed rather high uptake in the kidneys, a pharmacokinetic (PK) issue which may stem from physiological solubility.[15] Therefore, we sought to transform the bisaryl urea pharmacophore of **1** to a conformationally constrained 2-

arylaminobenzimidazole system to exploit benzimidazole-mediated physicochemical properties – in particular its extensive pi-orbital system, combination of hydrogen bond acceptors/donors, polarity, and relative acidity of the 2-aminobenzimidazole N-H proton (pKa = 6.4-7.5).[16,17] The latter three factors combine to improve aqueous solubility and possibly improve PK while alleviating kidney uptake. Indeed, these physicochemical properties of benzimidazoles result in diverse pharmaceutical applications addressing a variety of ailments,[18-25] making it an important member of the class of heterocycles having heteroatoms at the 1- and 3-positions.[26] As a consequence, *N*-aryl-2-aminobenzimidazoles facilitate favorable pharmacodynamics and pharmacokinetics (PK), thereby making them ideal components of drug candidates.[23,25] Herein, we report the design and synthesis - employing solution- and solid-phase chemistries - of benzimidazole analogs **2-10** (KLCA1-9), with the solubility measured by computational and analytical methods, and the potency of which were evaluated by cell adhesion competitive inhibition assays.

Results and Discussion

Chemistry. To aid in designing rational analogs, continuum-solvent quantum mechanical calculations were performed on the urea **1** and the benzimidazole moieties of **7** and **10** to ensure that the bisaryl urea □ benzimidazole modification would not drastically change the spatial orientation of the highly potent **1**. Figure 2 shows the low energy and most polar solvated conformations of benzimidazoles **7** and **10** juxtaposed to the bisaryl urea moiety of **1**. Indeed, while the number of rotatable bonds is decreased in the benzimidazole moiety, its aryl rings tend to have a staggered orientation that is similar to the urea moiety of **1** therefore making the bisaryl urea □ benzimidazole modification spatially tolerable. For **7**, the 2-arylaminobenzimidazole moiety has two low energy conformations and a rotamer around the amide carbonyl. Several low energy conformations exist for **10**: the 2-arylamino N-H as well as the 3-benzimidyl N-H are able to exist in either syn/anti geometries with the o-tolyl moiety in a staggered conformation and placement of the carboxamide occurs in either in the 5- or 6- positions. Furthermore, the energy difference between *syn*/*anti* geometries of the 2-arylamino N-H and the 3-benzimidyl N-H are

small and therefore able to meet the binding demands of the integrin. Most interestingly, the benzimidazole moiety has a larger dipole moment than the urea moiety of **1** leading to complete water solubility. These computational quantum calculations revealed that a bisaryl urea □ benzimidazole alteration does not cause a major change in spatial orientation of the aryl rings and that water solubility - based on dipole moment - is higher for the benzimidazole analogs thereby improving solubility and potentially PK.

With these computational studies in hand, we then focused on the preparation of the benzimidazole acid precursors. As depicted in Scheme 1, *m*- and *p*-aniline esters, either available commercially or prepared from a Fisher esterification of the corresponding aniline acid, were treated with thiophosgene to afford the respective aryl isothiocyanate ester **20a-e** in yields ranging from 89-93%. In a one-pot transformation, these aryl isothiocyante esters react with *o*-phenylenediamines to deliver unisolated thiourea intermediates, which subsequently cyclodesulferize in the presence of carbodiimide reagents delivering benzimidazole esters. Finally, saponification affords the *m*- and *p*-benzimidazole acids **11-19** in 71-84% yields from the aryl isothiocyanate ester and require minimal purification following workup, in part due to the high water solubility of the dianionic benzimidazole acid.[27] The acids derived from *o*-benzimidazole esters were not prepared due to the respective ester undergoing a 6-*exo*-trig cyclization to give the pharmaceutically interesting benzimidazoquinazolinone.[28]

With these *m*- and *p*-heterocyclic acids in hand, our focus turned to the synthesis of the target molecules **2-10**. As outlined in Scheme 2, Rink amino resin, prepared by first swelling Rink amide resin and then treatment with 20% piperidine/DMF, was treated with an activated amino acid solution (appropriately protected amino acid + DIC/HOBt in DMF). This process was repeated twice to yield the resin-bound tripeptide **21**. This resin was then divided into nine flasks and the heterocyclic acid precursors **11-19**, each dissolved in a solution of HBTU/DIEA in DMF, were added to the divided resin tripeptide **21** suspended in DMF. Protection of the electron deficient 2-arylaminobenzimidyl moiety was unnecessary as minimal polymerization occurred. Following reaction completion as judged by Kaiser test, the

heterocyclic tripeptide was cleaved from the solid support under acidic conditions (TFA/*i*Pr_3SiH/H_2O), and purified by reverse-phase HPLC to afford **2-10** in 50-71% overall yield from Rink amide resin and in 98-100% purity.

To further supplement the computational solubility results, our focuses turned to experimentally measuring solubility by determining the log*P* of the **2-10** analogs and contrasting these to **1** as shown in Figure 3a (see Supporting Information for tabulated values). The partition coefficient *P* is defined as the concentration of a compound in octanol over the concentration of the same substance in water.[29,30] The hydrocarbon-water partition coefficient *P* can be related to the experimentally determined capacity factor *k* by measuring the retention time of the compound using reverse-phase HPLC.[31,32] A standard calibration curve was determined using compounds with known log*P* values[33,34] and, after calculation of the capacity factor, the extrapolated log*P* values for **2-10** and **1** shown in Table 1 and the graph in Figure 3a indicate that all of the **2-10** compounds are appreciably more soluble than **1**.

Biological Evaluation. Integrin expression and function mediate cell activation and changes in integrin affinity, avidity, or activation state are implicated in cell migration, apoptosis, cancer development and metastasis.[35] Morever, $\alpha_4\beta_1$ integrin mediates cell adhesion to vascular cell adhesion molecule-1 (VCAM-1 or CD 106) as well as to extracellular matrix protein fibronectin.[4] We measured binding affinities (IC_{50}) of **2-10** in a Molt-4 T-cell leukemia adhesion assay by inhibiting the $\alpha_4\beta_1$-mediated cell adhesion to CS-1 peptide (DELPQLVTLPHPNLHGPEILDVPST), which is derived from the binding site of fibronectin to activated $\alpha_4\beta_1$ receptor.

We prepared 96-well plates by coating them with neutravidin, followed by adding biotin-conjugated CS-1 peptide. The wells were then blocked with BSA in PBS solution, followed by adding Molt-4 cells, and finally the addition of serially diluted **2-10** to each well. The plates were incubated, washed (PBS), fixed (formalin) and stained (crystal violet). After washing and drying at room temperature, the absorbance at 570 nm was measured using a UV/Vis spectrophotometer equipped to read 96-well plates. Inhibition was calculated as a percentage resulting from the concentration-dependent curve, and the IC_{50}

data is shown in Table 1. The IC_{50} of **1** was previously reported to be 2 pM with Jurkat cells.[14] The IC_{50} value tends to vary somewhat with different batch of cells and the specific cell line used. We used Molt-4 cells, instead of Jurkat cells, for our current binding studies because Molt-4 xenograft can be readily induced in nude mice and therefore will be used in our future in vivo pharmacokinetic and imaging studies. The IC_{50} of **1**, in this current study, was determined to be 37 pM, and this value will be used for comparison with that of the benzimidazole compounds.

The potency of the 4^7-methylbenzimidazole acetamide **9**, the compound that is most structurally similar to **1**, is in the low nanomolar range (IC_{50} = 28 nM; see Supporting Information for **2-10** structures). The SAR data indicates that removing the methylene unit as exemplified in the 4^7-methylbenzimidazole carboxamide **8** leads to a 23-fold decrease in potency (with respect to **9**). While holding the carboximide unit constant, removal of the 4^7-methyl (**7**; 15-fold decrease), reversing the benzimidyl and phenyl moieties (**10**; 14-fold decrease), and *m*-orientation of the carboxamide (**2**; 7-fold decrease) all were frivolous at increasing potency. Extending the methylene chain exemplified in the unsubstituted propanamide (**6**; 12-fold decrease) or the substituted 2-methylpropanamide (**3**; 16-fold) was also ineffective at improving potency. Returning to the acetamide, changing from 4^7- to 5^6-substitution as depicted by the 5^6-bromobenzimidazole acetamide (**4**; 12-fold decrease) was futile, however removing substitution altogether as shown in **5** lead to an 11-fold increase in potency into the picomolar range (IC_{50} = 305 pM) as shown in Figure 3b. While the bisaryl urea of **1** did have *o*-tolyl substituion, the unsubstituted benzimidazole **5** proved to be the most potent of this new class of compunds. This process of heterocyclization has two consequences: reducing a degree of rotational freedom reduces flexibility and/or accessibility of the acceptor which may account for the 8-fold decrease in potency into the low picomolar range with respect to **1**. However, heterocyclizing of the bisaryl urea pharmacophore to a conformationally constrained 2-arylaminobenzimidazole pharmacophore yields a more water soluble compound thanks to the acidity of the 2-arylamino N-H and a higher dipole moment which may in turn lead to improved PK.

Conclusion

The SAR data derived from the benzimidazole analogs differ from the previously reported SAR data of **1**[14] in that substitution at the R^1, R^2, or R^3 positions of the analogs was ineffective at increasing potency. However, **5** (IC_{50} = 305 pM) is still in the low picomolar range and potent enough to sustain in vivo selectivity, in addition to having a higher dipole moment, a more acidic N-H proton, and subsequently a lower log*P* value rendering **5** more water soluble than **1**. Using computational, synthetic, and analytical chemistries, in conjunction with a cell adhesion assay, we have successfully modified **1** from a bisaryl urea to a novel, highly water soluble 2-arylaminobenzimidazole **5** while maintaining picomolar potency as an antagonist for activated $\alpha_4\beta_1$ integrin. Subtle changes in the structure of a compound lead to enhanced physicochemical properties (dipole moment and pK_a) that result in increased solubility (log*P*), which is an important factor with potential to improve PK. Given the history of successful benzimidazole drug candidates, this transformation has the potential to allow for improved PK without sacrificing potency or selectivity to aid in diagnosing/treating patients with lymphoma. In vivo therapeutic and imaging studies on lymphoid malignancies are under study and will be reported in due course.

Experimental Section

General Procedure for Aryl Isothiocyanate Esters: Ethyl 4-Isothiocyanatobenzoate (20a). Following our previously reported procedure,[27] a solution of an appropriate aniline ester (4.5 g, 27.3 mmol) and triethylamine (60.1 mmol, 8.37 mL) in ethyl acetate (160 mL), was treated with thiophosgene (30.0 mmol, 2.30 mL) in ethyl acetate (130 mL) dropwise over 30 min at 0 ºC. After addition, the cooling bath was removed and the reaction mixture was allowed to gradually warm up to room temperature over 12 h. The workup consisted of diluting with ethyl acetate, followed by washing sequentially with water (200 mL x 2) and brine (200 mL). The organic layer was dried ($MgSO_4$), concentrated, and the crude product was purified via short path CC (hexanes/ethyl acetate, 9:1) to give **20a** (5.03 g, 89%). The analytical data are in accord with literature values.[36]

General Procedure for Benzimidazole Acids: 3-(1*H*-Benzo[*d*]imidazol-2-ylamino)benzoic Acid (11). Following our previously reported procedure,[27] to a solution of *o*-phenylenediamine (1.76 g, 16.3

mmol) in CH_2Cl_2 (75 mL) was added a solution of the aryl isothiocyanate ester (For **20a**, 3.0 g, 15.5 mmol) in CH_2Cl_2 (75 mL) dropwise over 30 min, followed by stirring for 16 h at room temperature. After TLC showed that the aryl isothiocyanate was consumed, the appropriate carbodiimide reagent [1,3-diisopropylcarbodiimide (DIC) or *N*-(3-dimethylaminopropyl)-*N'*-ethylcarbodiimide hydrochloride (EDCI)] was added (for **11**, DIC (46.5 mmol, 7.2 mL)), and the reaction proceeded at room temperature until TLC showed the intermediate thiourea was consumed. In most instances, this was between 4-8 h., but in some cases this took as long as 16 h (**11**, 6 h). If DIC was employed (**11**) the concentrated crude product was recrystallized from hot $CHCl_3$ and petroleum ether to give the benzimidazole ester (3.67 g). If EDC was utilized, then the residue was taken up in ethyl acetate/H_2O followed by washing (H_2O, brine), drying ($MgSO_4$), and concentration to give the benzimidazole ester (4.08 g) which was used without further purification. A solution of the benzimidazole ester (4.08 g, 15.3 mmol) in dioxane/H_2O (125 mL/80 mL) was treated with LiOH (1.83 g, 76.4 mmol) and the solution was refluxed for 16 h. The reaction mixture was concentrated, and the residue was taken up in aqueous 2 M NaOH. This basic water layer (pH ~10) was washed twice with ether before being acidified with concentrated HCl to pH ~2-3 at which point **11** precipitated as a white solid (3.38 g, 86 %). The analytical data are in accord with literature values.[37]

H_2N-K[(*E*)-3-(pyridin-3-yl)acrylamide]-Aad(O*t*Bu)-Ach-Rink Polystyrene (21). Rink amide resin (2.35 g, 1.19 mmol) was swollen in DMF (30 mL) for 3 h, followed by treatment with 20% piperidine in DMF (20 mL). After washing, the resin was then treated with a pre-mixed solution of Fmoc-Ach-OH (Fmoc-Ach-OH; 1.30 g, 3.57 mmol), 1,3-diisopropylcarbodiimide (DIC; 3.57 mmol, 553 μL), and hydroxybenzotriazole (HOBt; 482 mg, 3.57 mmol) in DMF (20 mL) followed by shaking for 6 h. After a negative Kaiser test[38] washing, this sequence of deprotection/coupling was repeated thrice more with Fmoc-Aad(*t*Bu)-OH (1.57 g, 3.57 mmol), Dde-K(Fmoc)-OH (1.85 g, 3.57 mmol), and (*E*)-3-(pyridin-3-yl)acrylic acid (532 mg, 3.57 mmol). After washing, the Dde-tripeptide resin was washed and treated with 2% H_2NNH_2 in DMF (20 mL) for 20 min, followed by washing to afford the free amino-tripeptide

resin **21**: IR (neat) 3430 (sh), 3370 (sh), 3084, 1740 (st), 1684 (st), 1680 (st), 1662 (st), 1654 (st) cm^{-1}.

General Procedures for Benzimidazole Analogs: (*R*)-5-((*R*)-2-(3-(1*H*-Benzo[*d*]imidazol-2-ylamino)benzamido)-6-((*E*)-3-(pyridin-3-yl)acrylamido)hexanamido)-6-(1-carbamoylcyclohexyl-amino)-6-oxohexanoic Acid (2). Benzimidazole acid **11** (253 mg, 0.180 mmol), 2-(1*H*-benzotriazole-1-yl)-1,1,3,3-tetramethyluronium hexafluorophosphate (HBTU; 67 mg, 0.180 mmol), and DIEA (54.7 mL, 0.360 mmol) were dissolved in DMF (3 mL) and the homogenous solution was allowed to stand for 10 min. This solution was then added to the free amino tripeptide resin **21** (120 mg, 0.06 mmol) and was shaken for 4 h. After washing, the resin was then cleaved with 3 mL of a 95:2.5:2.5 cleavage solution of TFA:H_2O:TIPS for 2 h, followed by draining and washing with the cleavage solution. This cleavage process was repated once more, and the combined filtrates were concentrated under a gentle stream of nitrogen, precipitated with ether, centrifuged, and decanted. The precipitate was then purified by preparatory HPLC, and the combined fractions were lyophillized to afford **2** (29 mg, 63 % from Rink Amide resin) as a white powder: ESI MS (*m/z*) 780 $(M + H)^+$; MALDI HRMS (*m/z*) for $C_{41}H_{50}N_9O_7$: Calcd. 780.3828 $(M + H)^+$. Found: 780.3835. Purity was determined to be 99% by HPLC analysis on the basis of absorption at 220 nm. This procedure for was used **3-10** and analytical data are shown in Table 2.

Acknowledgements. The authors thank the Howard Hughes Medical Institute-Integrating Medicine into Basic Science Fellowship Program, National Cancer Institute (CA113298), the National Institute for General Medical Sciences (RO1-GM076151), and the National Science Foundation (NMR spectrometers; CHE-0443516 and CHE-9808183) for their generous financial support. This work was in part performed under the auspices of the United States Department of Energy by the University of California, Lawrence Livermore National Laboratory under contract number W-7405-ENG-48.

Supporting Information Available: Structures and analytical data for **1-10** and precursors **11-21** are provided in addition to cell adhesion assay graphs. This material is available free of charge via the Internet at http://pubs.acs.org.

References

1. Lin, K. C.; Castro A. C. Very late antigen 4 (VLA4) antagonists as anti-inflammatory agents. *Curr. Opin. Chem. Biol.* **1998**, *2*, 453-457.

2. Yusut-Makagiansar H.; Anderson M. E.; Yakovleva T. V.; Murray J. S.; Siahaan T. J. Inhibition of LFA-1/ICAM-1 and VLA-4/VCAM-1 as a therapeutic approach to inflammation and autoimmune diseases. *Med Res. Rev.* **2002**, *22*, 146-167.

3. Holzman B.; Gosslar U.; Bittner M. α_4 integrins and tumor metastasis. *Curr. Top. Microbiol. Immunol.* **1998**, *231*, 125-141.

4. Vincent A. M.; Cawley J. C.; Burthem J. Integrin function in chronic lymphocytic leukemia. *Blood* **1996**, *87*, 4780-4788.

5. Marco, R. A.; Diaz-Montero, C. M. Wygant, J. N.; Kleinerman, E. S.; McIntyre, B. W. Alpha 4 integrin increases anoikis of human osteosarcoma cells. *J. Cell. Biochem.* **2003**, *88*, 1038-1047.

6. de la Fuente, M. T.; Casanova, B.; Garcia-Gila, M.; Silva, A.; Garcia-Pardo, A. "Fibronectin interaction with alpha4beta1 integrin prevents apoptosis in B cell chronic lymphocytic leukemia: correlation with Bcl-2 and Bax." *Leukemia* **1999**, *13*, 266-274.

7. Oldon, D. L.; Burkly, L. C.; Leone, D. R.; Dolinski, B. M.; Lobb, R. R. Anti-alpha4 integrin monoclonal antibody inhibits multiple myeloma growth in a murine model. *Mol. Cancer Ther.* **2005**, *4*, 91-99.

8. Matsunaga T.; Takemoto N.; Sato, T.; Takimoto, R.; Tanaka, I.; Fujimi, A.; Akiyama, T.; Kuroda, H.; Kawano, Y.; Kobune, M.; Kato, J.; Hirayama, Y.; Sakamaki, S.; Kohda, K.; Miyake K.; Niitsu Y. Interaction between leukemic-cell VLA-4 and stromal fibronectin is a decisive factor for minimal residual disease of acute myelogenous leukemia. *Nat. Med.* **2003**, *9*, 1158-1165.

9. Garmy-Susini, B.; Jin, H.; Zhu, Y.; Sung, R-J.; Hwang, R. Varner, J. Integrin alpha4beta1-VCAM-1-mediated adhesion between endothelial and mural cells is required for blood vessel maturation. *J. Clin. Invest.* **2005**, *115*, 1542-1551.

10. Damiano, J. S.; Dalton, W. S. Integrin-mediated drug resistance in multiple myeloma. *Leuk. Lymphoma* **2000**, *38*, 71-81.

11. Lam, K. S.; Salmon, S. E.; Hersh, E. M.; Hruby, V. J.; Kazmierski, W. M.; Knapp, R. J. A new type of synthetic peptide library for identifying ligand-binding activity. *Nature* **1991**, *354*, 82-84.

12. For an OBOC review see: Lam, K.S.; Lebl M.; Krchnak V. The ''one-bead-one-compound'' combinatorial library method. *Chem. Rev.* **1997**, *97*, 411-448.

13. Chen X.; Gambhir S. S. Significance of one-bead-one-compound combinational chemistry. *Nature Chem. Bio.* **2006**, *2*, 351-352.

14. Peng L.; Liu R.; Marik J.; Wang X.; Takada Y.; Lam K. S. Combinatorial chemistry identifies high-affinity peptidomimetics against $\alpha_4\beta_1$ integrin for *in vivo* tumor imaging. *Nat. Chem. Biol.* **2006**, *2*, 381-389.

15. Lin, K.-c.; Ateeq, H. S.; Hsiung, S. H.; Chong, L. T.; Zimmerman, C. N.; Castro, A.; Lee, W.-c.; Hammond, C. E.; Kalkunte, S.; Chen, L.-L.; Pepinsky, R. B.; Leone, D. R.; Sprague, A. G.; Abraham, W. M.; Gill, A.; Lobb, R. R.; Adams, S. P. Selective, Tight-Binding Inhibitors of Integrin $\alpha_4\beta_1$ That Inhibit Allergic Airway Responses. *J. Med. Chem.* **1999**, *42*, 920-934.

16. Perkins, J. J.; Zartman, A. E.; Meissner, R. S. Synthesis of 2-(alkylamino)benzimidazoles. *Tetrahedron Lett.* **1999**, *40*, 1103-1106.

17. (a) Hajduk, P. J.; Boyd, S.; Nettesheim, D.; Nienaber, V.; Severin, J.; Smith, R.; Davidson, D.; Rockway, T.; Fesik, S. W. Identification of Novel Inhibitors of Urokinase via NMR-Based Screening. *J. Med. Chem.* **2000**, *43*, 3862-3866. (b) Schilling, S.;; Niestroj, A. J.; Rahfeld, J.-U.;

Hoffmann, T.; Wermann, M.; Zunkel, K.; Wasternack, C.; Demuth, H.-U. Identification of Human Glutaminyl Cyclase as a Metalloenzyme: Potent inhibition by imidazole derivatives and heterocyclic chelators. *J. Biol. Chem.* **2003**, *278*, 49773-49779.

18. Janssens, F.; Torremans, J.; Janssen, M.; Stokbroekx, R. A.; Luyckx, M.; Janssen, P. A. New antihistaminic N-heterocyclic 4-piperidinamines. 1. Synthesis and antihistaminic activity of N-(4-piperidinyl)-1H-benzimidazol-2-amines. *J. Med. Chem.* **1985**, *28*, 1925-1933.

19. Bovet, D.; Bovet-Nitti, F. "Medicaments du Systeme Nerveux Vegetatif"; Karger, 5th, ed.; Basel, 1948; p 741.

20. Wade, A., Ed. "The Extra Pharmacopeia", 27th ed; The Pharmaceutical Press: London, 1978; pp 1287-1309.

21. Chong, C. R.; Chen, X.; Shi, L.; Liu, J. O.; Sullivan, D. J. A clinical drug library screen identifies astemizole as an antimalarial agent. *Nature Chem. Bio.* **2006**, *2*, 415-416.

22. Wright, D. H.; Ford-Hutchinson, A. W.; Chadee, K.; Metters, K. M. The human prostanoid DP receptor stimulates mucin secretion in LS174T cells. *Br. J. Pharmacol.* **2000**, *131*, 1537-1545.

23. Arimura, A.; Yasui, K.; Kishino, J.; Asanuma, F.; Hasegawa, H.; Kakudo, S.; Ohtani, M.; Arita, H. Prevention of allergic inflammation by a novel prostaglandin receptor antagonist, S-5751. *J. Pharm. Exp. Ther.* **2001**, *298*, 411-419.

24. Beaulieu, C.; Wang, Z.; Denis, D.; Greig, G.; Lamontagne, S.; O'Neill, G.; Slipetz, D.; Wang, J. Benzimidazoles as new potent and selective DP antagonists for the treatment of allergic rhinitis. *Bioorg. Med. Chem. Lett.* **2004**, *14*, 3195-3199.

25. Rastogi, R.; Sharma, S. 2-Aminobenzimidazoles in Organic Syntheses. *Synthesis* **1983**, 861-882.

26. Martin, E. J.; Critchlow, R. E. Beyond Mere Diversity: Tailoring Combinatorial Libraries for Drug Discovery. *J. Comb. Chem.* **1999**, *1*, 32-45.

27. Carpenter, R. D.; DeBredt, P. B.; Lam, K. S.; Kurth, M. J. Carbodiimide-Based Benzimidazole Library Method. *J. Comb. Chem.* **2006**, *8*, 907-914.

27. Carpenter, R. D.; Lam, K. S.; Kurth, M. J. Microwave-Mediated Heterocyclization to Benzimidazo[2,1-b]quinazoline-12(5*H*)-ones. *J. Org. Chem.* **2007**, *72*, 284-287.

28. Malik, I. Sedlarova, M. A.; Csollei, C. S.; Andrianainty, P.; Kurfurst, P.; Vanco, J. Synthesis, spectral description, and lipophilicity parameters determination of phenylcarbamic acid derivatives with integrated N-phenylpiperazine moiety in the structure. *Chem. Pap.* 2006, 60, 42-47.

29. Saunders, R. A.; Platts, J. A. Scaled polar surface area descriptors: Development and application to three sets of partition coefficients. New J. Chem. 2004, 28, 166-172.

30. Bechalany, A.; Tsantili-Kakoulidou, A.; El Tayar, N.; Testa, B. Measurement of lipophilicity indices by reversed-phase high-performance liquid chromatography: comparison of two stationary phases and various eluents. J. Chromatogr. 1991, 541, 221-229.

31. Braumann, T. Determination of hydrophobic parameters by reversed-phase liquid chromatography: theory, experimental techniques, and application in studies on quantitative structure-activity relationships. *J. Chromatogr.* **1986**, *373*, 191-225.

32. Vrakas, D.; Tsantili-Kakoulidou, A.; Hadjipavlou-Litina, D. Exploring the consistency of logP estimation for substituted coumarins. *QSAR & Comb. Sci.* **2003**, *22*, 622-629.

33. Poole, S. K.; Poole, C. F. Separation methods for estimating octanol-water partition coefficients. *J. Chromatogr. B.* **2003**, *797*, 3-19.

34. Luscinskas F.; Lawler, J. Integrins as dynamic regulators of vascular function. *FASEB J.* **1994**, *8*, 929-938.

35. Sayigh, A. A. R.; Ulrich, H.; Potts. J. S. The Reaction of Arylamines with Diethylthiocarbamoyl Chloride. A New Synthesis of Aryl Isothiocyanates. *J. Org. Chem.* **1965**, *30*, 2465-2466.

36. Jacobsen, C. M.; Denmeade, S. R.; Isaacs, J. T.; Gady, A.; Olsen, C. E.; Christensen, S. B. Design, Synthesis, and Pharmacological Evaluation of Thapsigargin Analogues for Targeting Apoptosis to Prostatic Cancer Cells. *J. Med. Chem.* **2001**, *44*, 4696-4703.

37. Kaiser, E.; Colescott, R. L.; Bossinger, C. D.; Cook, P. I. Color test for detection of free terminal amino groups in the solid-phase synthesis of peptides. *Anal. Biochem.* **1970**, *34*, 595-598.

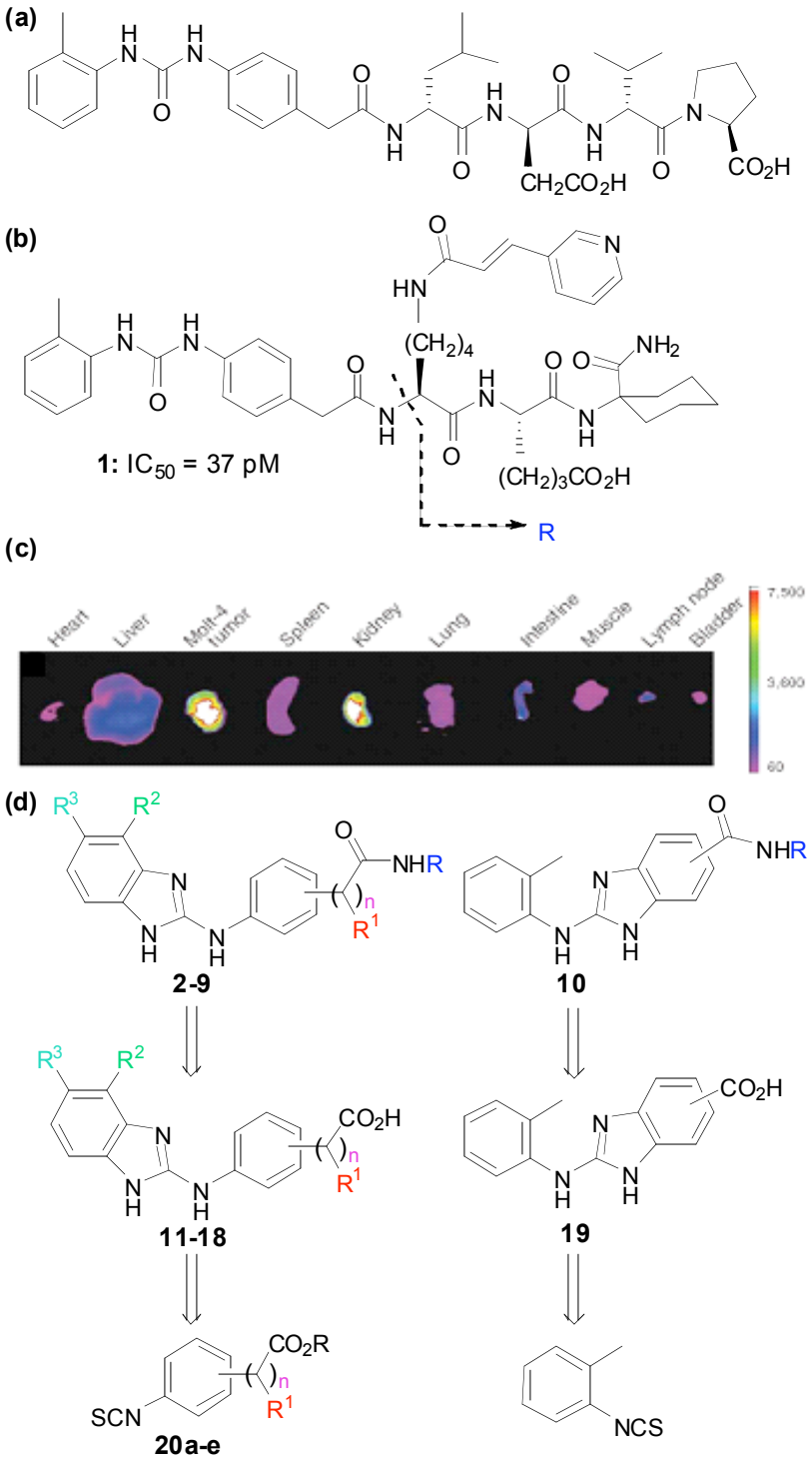

2 & 11: *m*-, n = 0, $R^1 = R^2 = R^3 = H$
3 & 12: *p*-, n = 1, $R^2 = R^3 = H$, $R^1 = CH_3$
4 & 13: *p*-, n = 1, $R^1 = R^2 = H$, $R^3 = Br$
5 & 14: *p*-, n = 1, $R^1 = R^2 = R^3 = H$
6 & 15: *p*-, n = 2, $R^1 = R^2 = R^3 = H$
7 & 16: *p*-, n = 0, $R^1 = R^2 = R^3 = H$
8 & 17: *p*-, n = 1, $R^2 = CH_3$, $R^1 = R^3 = H$
9 & 18: *p*-, n = 0, $R^2 = CH_3$, $R^1 = R^3 = H$

Figure 1. **(a)** Structure of Bio-1211;[15] **(b)** Structure of **1** (IC_{50} 37 pM); **(c)** *Ex vivo* NIRF images of tumors and organs excised 24 h after postinjection with **1**-streptavidin-Alexa680 biotin;[14] **(d)** Structure, retrosynthetic analysis, and diversity elements of benzimidazoleanalogs.

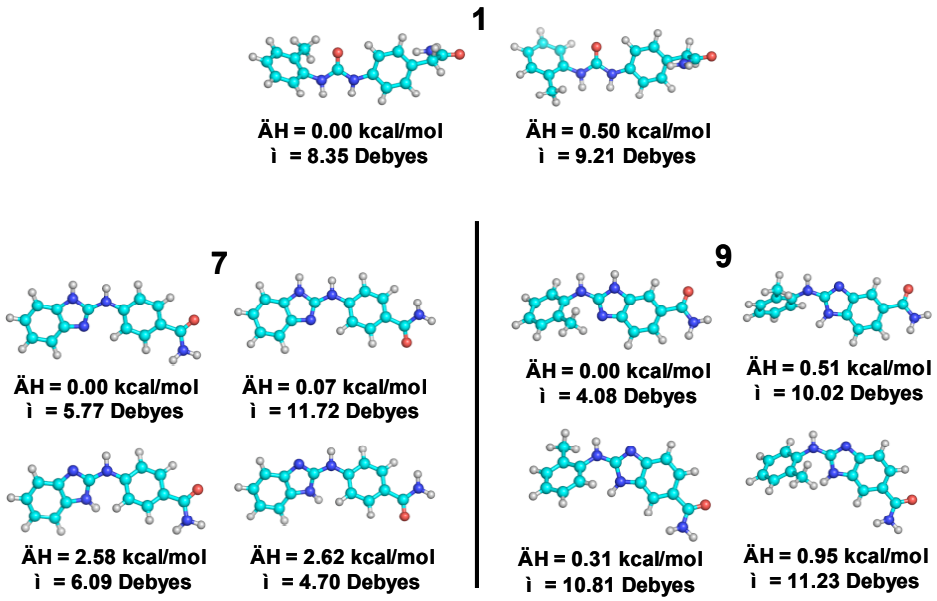

Figure 2. Conformational analysis, (ΔH, energy difference between shown structure and lowest energy structure) and dipole moment (μ) solution-phase calculations for the bisaryl urea moiety of **1** and benzimidazoles **7** and **9**.

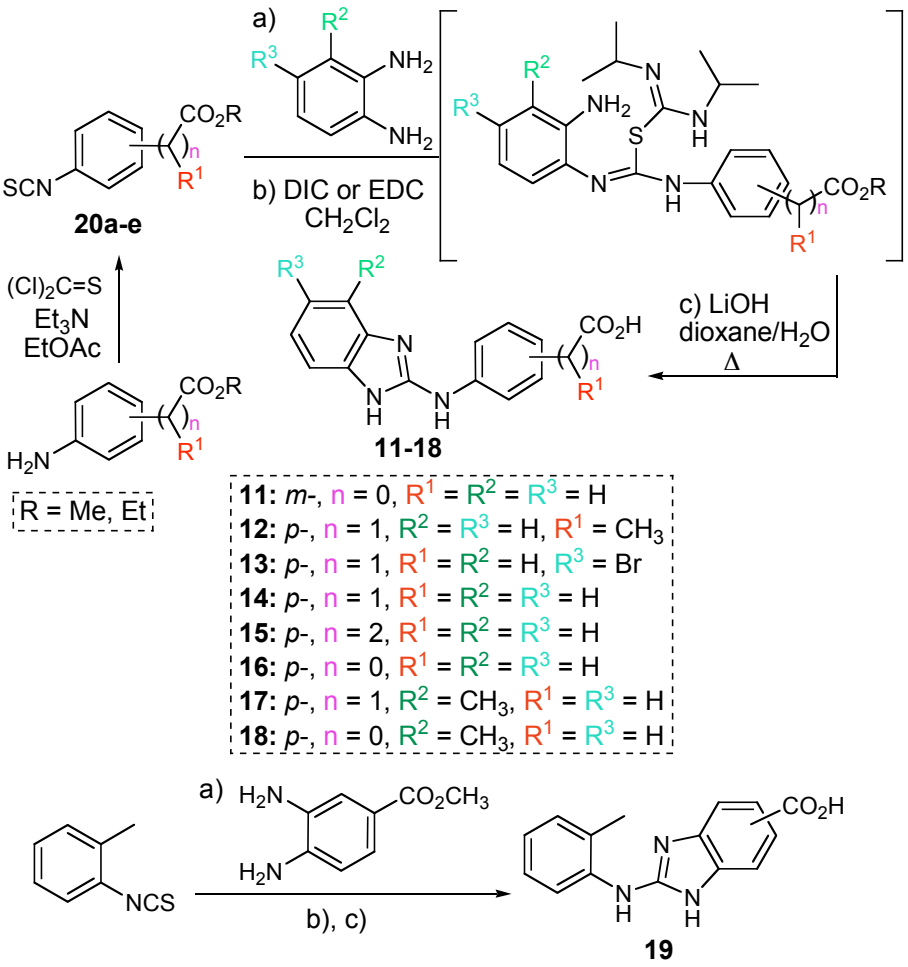

Scheme 1. Synthetic route to *m*-/*p*-benzimidazole acid precursors via an amidine thiocarbonate intermediate.

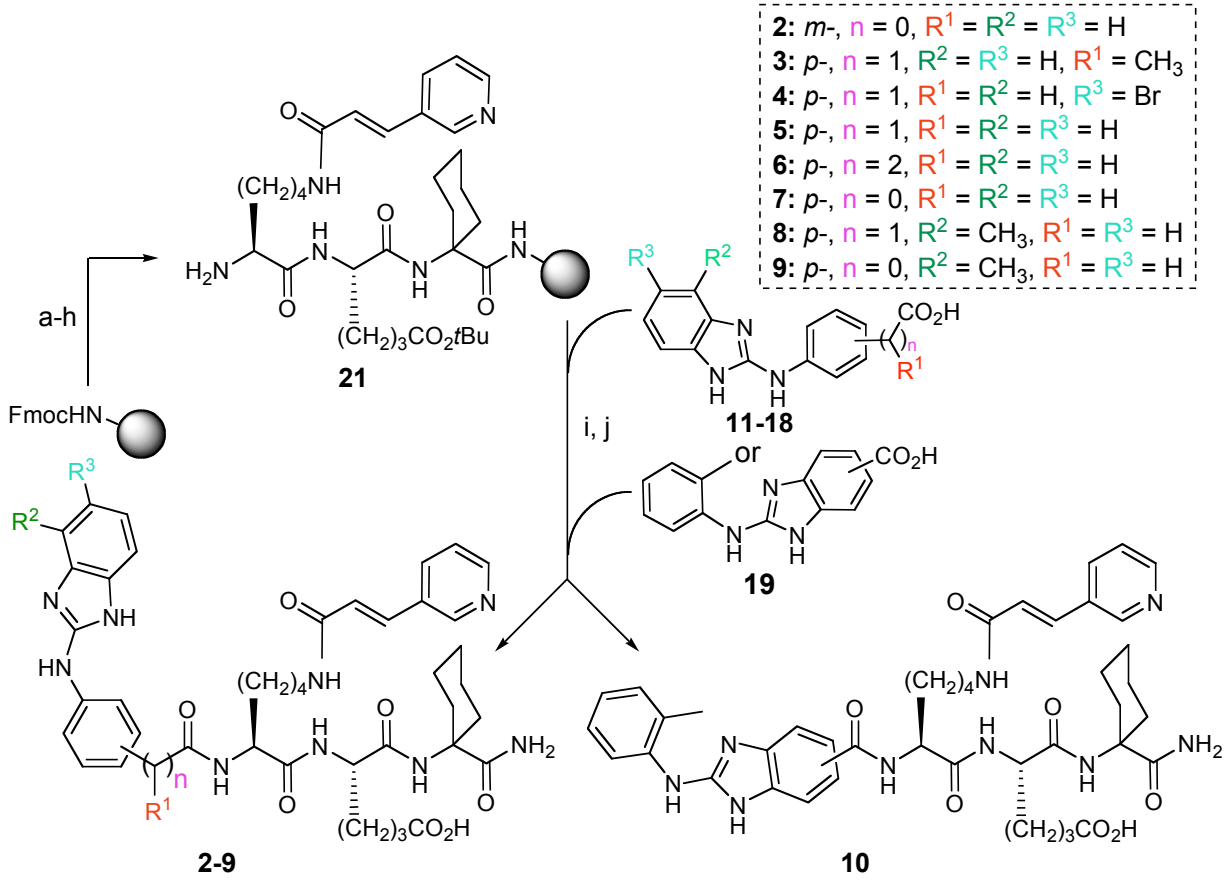

Scheme 2. (a) swell/DMF, 3h; (b) piperidine/DMF; (c) Fmoc-Ach-OH, DIC, HOBt, DMF; (b)□(e). Fmoc-Aad(O*t*Bu)-OH, DIC, HOBt, DMF; (b)□(f) Dde-K(Fmoc)-OH, DIC, HOBt, DMF; (b)□(g) (*E*)-3-(pyridin-3-yl)acrylic acid, DIC, HOBt, DMF; (h) H_2NNH_2/DMF; (i) **11-18** or **9** HBTU, EtN(*i*Pr)$_2$, DMF; (j) TFA, (*i*Pr)$_3$SiH, H_2O.

Table 1. Overall yield, purity, $[M + H]^+$ peak, experimentally determined log*P*, and IC_{50} of **2-10**.

Compound	Yield	Purity	$(M + H)^+$	log*P* (exptl)	$IC_{50} \pm SD$
1	--	--	--	3.26	37.2 ± 24.3 pM
2	63 %	100 %	780	2.12	185.6 ± 74.79 nM
3	60 %	98 %	808	2.63	444 ± 26.8 nM
4	57 %	100 %	872, 874	1.96	340 ± 23.33 nM
5	62 %	99 %	794	2.23	305 ± 58 pM
6	71 %	98 %	808	2.80	344 ± 266 nM
7	64 %	98 %	780	1.83	419.5 ± 333 nM
8	59 %	99 %	794	1.86	655 ± 79 nM
9	53 %	98 %	808	2.58	27.5 ±1.76 nM
10	50 %	99%	794	1.88	379 ± 138.5 nM

(a)

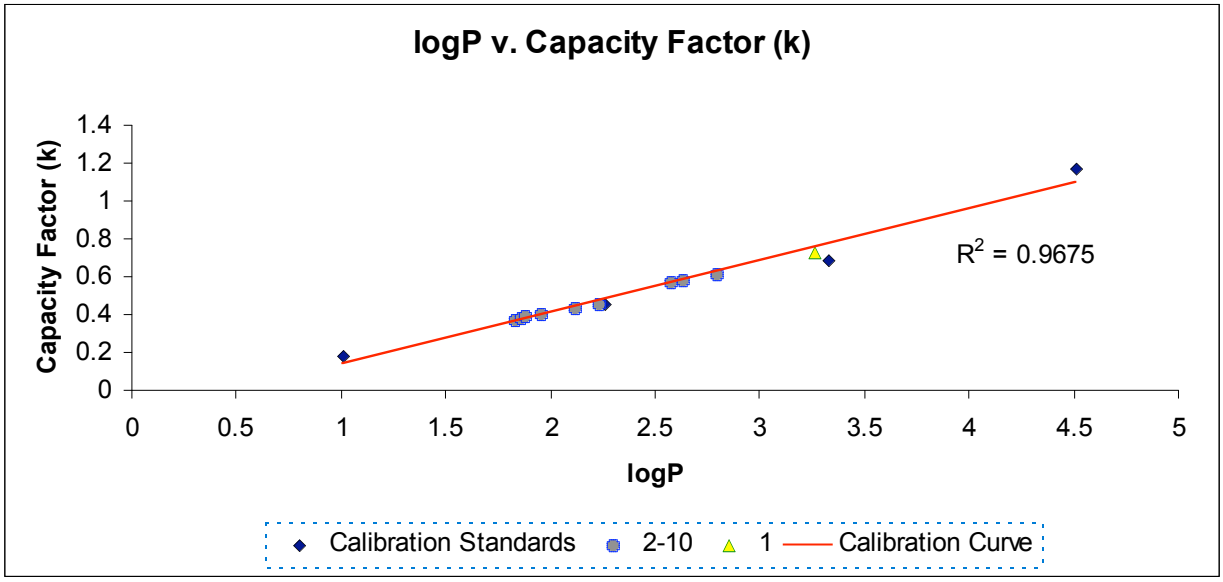

Figure 3. (a) Graph of log*P* vs. Capacity Factor (*k*) for **1-10** (see Supporting Information for values); (b) Chemical structure of **5** and its inhibitory effects on Molt-4 cell adhesion to immobilized CS-1 peptide. Based on the three cell adhesion inhibition curves (triplicate each), the IC_{50} was determined to be 305 $\pm$ 58 pM. (triplicates for each curve).

Table of Contents Graphic: